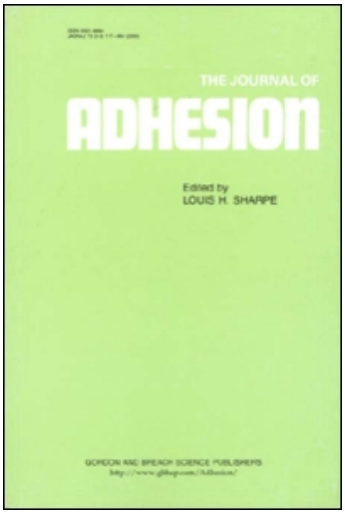

The Journal of Adhesion
Publication details, including instructions for authors and subscription information:
http://www.informaworld.com/smpp/title~content=t713453635

Parameter Governing Thin Film Adhesion-Delamination in the Transition from DMT- to JKR-Limit

Guangxu Li[a]; Kai-tak Wan[a]
[a] Mechanical and Industrial Engineering, Northeastern University, Boston, Massachusetts, USA

Online publication date: 27 October 2010

To cite this Article Li, Guangxu and Wan, Kai-tak(2010) 'Parameter Governing Thin Film Adhesion-Delamination in the Transition from DMT- to JKR-Limit', The Journal of Adhesion, 86: 10, 969 — 981
To link to this Article: DOI: 10.1080/00218464.2010.515470
URL: http://dx.doi.org/10.1080/00218464.2010.515470

The Journal of Adhesion, 86:969–981, 2010

ISSN: 0021-8464 print/1545-5823 online
DOI: 10.1080/00218464.2010.515470

Taylor & Francis
Taylor & Francis Group

Parameter Governing Thin Film Adhesion-Delamination in the Transition from DMT- to JKR-Limit

Guangxu Li and Kai-tak Wan
Mechanical and Industrial Engineering, Northeastern University, Boston, Massachusetts, USA

Professor David A. Dillard and his collaborators invented the constrained blister and the related punch test for characterizing thin film adhesion-delamination and the disjoining pressure at the interface of a clamped membrane and a rigid substrate. A new dimensionless parameter, $\psi_s = [6(1-\nu)a^4/\gamma^3 Eh]^{1/4}p$, relating the membrane dimensions (radius, a, and thickness, h), materials properties (elastic modulus, E, and Poisson's ratio, ν), and adhesion (interface energy, γ, and disjoining pressure, p), is shown to account for the transition from the long range surface force limit with small ψ (Derjaguin-Muller-Toporov, DMT) to the short range limit with large ψ (Johnson-Kendall-Roberts, JKR). This parameter serves as a flexible membrane counterpart to the classical Tabor's parameter for adhesion in bulk solids. An alternative form is defined for thick circular plate under bending, $\psi_b = [6(1-\nu)a^4/\gamma Eh^3]^{1/2}p$. Three case studies, namely, the standard pressurized blister, the constrained blister, and the punch tests are investigated for membranes under either pure bending or pure stretching deformations.

Keywords: Adhesion; Blister; Cohesive zone; JKR; Membrane

1. INTRODUCTION

Dillard *et al.* modified the classical pressured blister test and introduced the first constrained blister test [1–3]. In the standard blister test (Fig. 1a) invented by Dannenberg [4], hydrostatic or air pressure applied *via* a bore in the substrate drives an axisymmetric delamination along the membrane-substrate interface. A simple energy balance entails a catastrophic propagation once the delamination initiates, which is consistent with the many experimental evidences over

Received 19 December 2009; in final form 17 March 2010.
One of a Collection of papers honoring David A. Dillard, the recipient in 2010 of *the Adhesion Society Award for Excellence in Adhesion Science, Sponsored by 3M*.
Address correspondence to Kai-tak Wan, Northeastern University, SN334, 360 Huntington Avenue, Boston, MA 02115, USA. E-mail: ktwan@coe.neu.edu

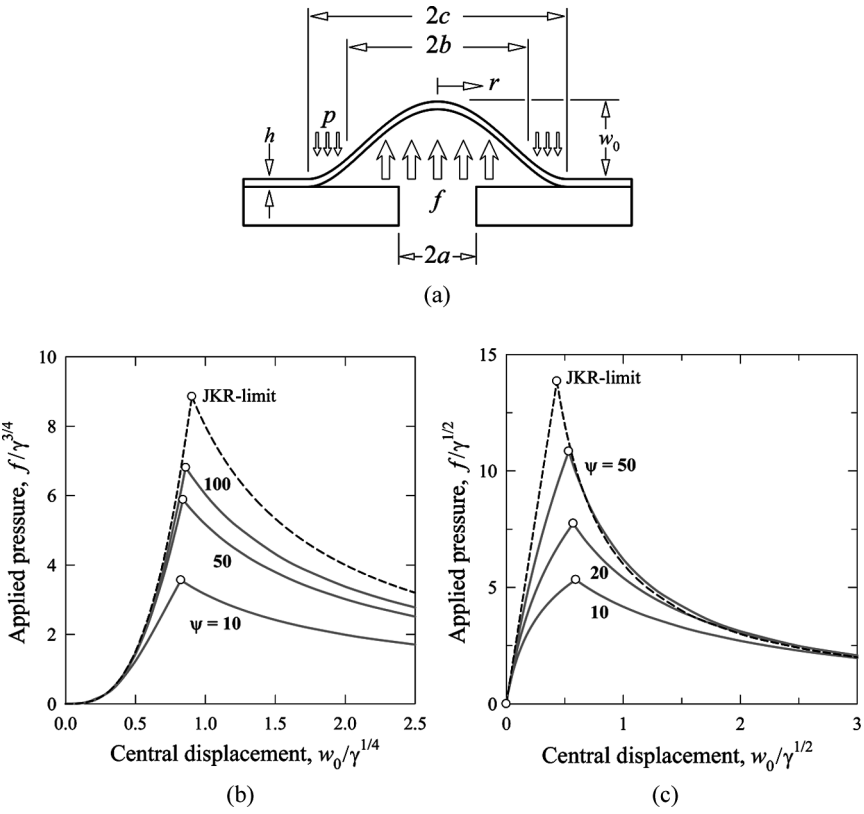

FIGURE 1 The standard pressurized blister test: (a) Setup; (b) Mechanical response for thin membrane under pure stretching; (c) Mechanical response for thin plate under pure bending. Delamination under either stretching or bending is fairly similar, in that a maximum load denoted by ○ indicates the onset of cohesive zone shrinkage.

the years [5]. The constrained blister test places a rigid plate above the membrane such that the blister height is limited and, thus, stabilizes the delamination process. Both the pressurized blister and constrained blister method lead to an expanding delamination front. Dillard *et al.* further modified the constrained blister by clamping a freestanding membrane at the periphery (Fig. 2a) [6]. Upon an external pressure, the membrane bulges and makes adhesion contact with the fixed plate above. As the pressure is made to decrease, the contact circle shrinks within a confined area. By measuring simultaneously the applied pressure and contact radius, the adhesion energy and the magnitude and range of the disjoining pressure can be measured.

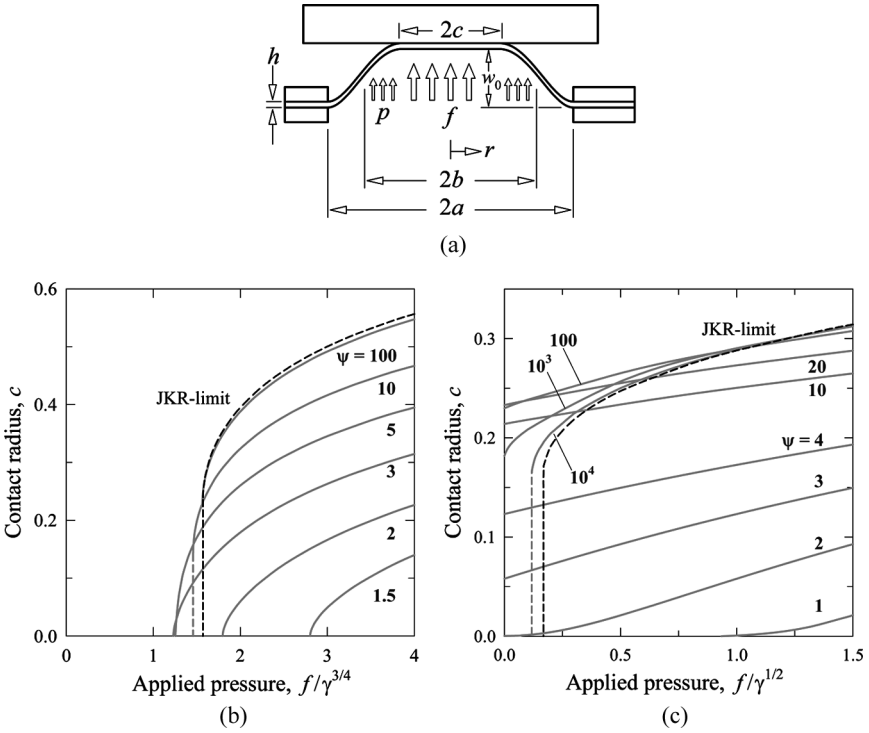

FIGURE 2 The constrained blister test: (a) Setup; (b) Mechanical response for thin membrane under pure stretching. Adhesion energy, $\gamma = 0.8$ and blister height, $w_0 = 0.8$; (c) Mechanical response for thin plate under pure bending. Adhesion energy, $\gamma = 0.22$ and blister height, $w_0 = 0.055$. The specific values of γ and w_0 are so chosen to be consistent with White's earlier calculation [17]. The dashed curve indicates the JKR-limit.

An alternative testing method is to replace the uniform pressure by a mechanical load to drive a delamination (Fig. 3a) known as the punch test [7,8]. A cylindrical punch makes contact with the clamped membrane, before a tensile force is applied to drive the delamination and, thus, to diminish the contact radius. Interfacial adhesion can be characterized by the mechanical response. The elegant techniques of constrained blister and punch tests are useful in many applications in electronics, biomedical sciences, and nano-technology whenever thin membranes are ubiquitous.

In our previous work, we have shown how the combination of magnitude and force range of the disjoining pressure or intersurface forces plays a crucial role in determining the mechanical response of the

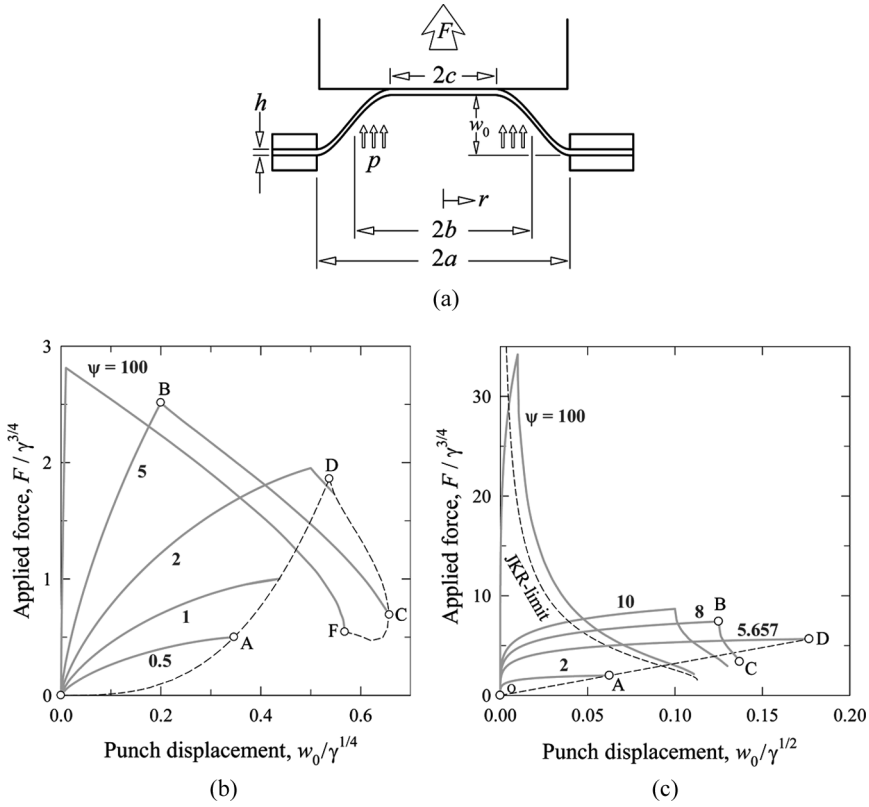

FIGURE 3 The punch test: (a) Setup; (b) Mechanical response for thin membrane under pure stretching. DMT-limit is exemplified by path OA, and JKR-limit by OF. Transition is seen along path OBC. The curve OADCF denotes the locus of "pinch-off" and "pull-off." (c) Mechanical response for thin plate under pure bending. DMT-limit is exemplified by path OA, and JKR-limit by the dashed curve. Transition is seen along path OBC that terminates at C. The curve OAD denotes the locus of pinch-off.

membrane upon delamination [9]. Before discussing membranes, we will first discuss the classical adhesion theory for bulk solids in the presence of intersurface forces [10,11]. When two identical elastic spheres with radius, R, elastic modulus, E, and Poisson's ratio, ν, adhere *via* an interfacial attraction such as electrostatic and van der Waals interactions, a non-zero contact circle is formed at the sphere-sphere interface. To circumvent the sophisticated mathematical feat to construct an adhesion mechanics model according to the Lennard-Jones potential, the classical Dugdale model is exploited, in

that, both the force range, y, and magnitude, p, are made constant but are constrained by the adhesion energy, $\gamma = py$, or area under the force-separation curve, $p(y)$. The Johnson-Kendall-Roberts (JKR) limit assumes an infinite p as y vanishes, while the Derjaguin-Muller-Toporov (DMT) limit takes the opposite extreme with a vanishing p but y tending to infinity. To account for the more realistic intermediate values of p and y, Tabor [12], Muller *et al.* [13], and Maugis [14] suggest the famous Tabor's parameter or its variants, $\mu = (16R\gamma^2/9K^2y^3)^{1/3}$, or $\mu = p(16R/9K^2\gamma)^{1/3}$ with $K = 2E/3(1-\nu^2)$. Rather than being just a numerical gauge, μ can be interpreted as a normalized magnitude of the disjoining pressure, $\mu = [4R(1-\nu^2)/\gamma E^2]^{1/3}p$. In general, the JKR limit is valid for $\mu > 2$ and the DMT limit for $\mu < 0.1$, and the intermediate values of μ lead to a JKR-DMT transition. Experimentally, the two limits have distinct characteristics at "pull-off", namely, a non-zero contact radius at the JKR limit but a zero contact at the DMT limit. Adhesion maps showing different regimes of adhesion behavior as functions of applied load and Tabor's parameter fills the literature [15].

Though successful, the JKR-DMT transition model and the Tabor's parameter are inadequate to discuss thin membranes where mixed plate-bending and membrane-stretching, rather than compressive stress as in bulk solids, dominate the elastic deformation. Dillard *et al.* extend the solid-solid adhesion model to thin film delamination in the constrained blister test by replacing the line force at the delamination front by a cohesive zone of finite width [6]. In this paper, we

TABLE 1 Normalized Coordinates and Variables

	Physical parameters (bold)	Normalized parameters
Geometrical parameters	$\boldsymbol{w_0}$ = blister height	$w_0 = \boldsymbol{w}_0/\boldsymbol{h}$
	$\boldsymbol{a}$ = membrane radius (or hole radius in standard pressurized blister test)	$c = \boldsymbol{c}/\boldsymbol{a}$
	$\boldsymbol{c}$ = radius of contact circle	$b = \boldsymbol{b}/\boldsymbol{a}$
	$\boldsymbol{b}$ = radius of cohesive edge	
	$\boldsymbol{h}$ = membrane thickness	
Material parameters	ν = Poisson's ratio	$\gamma = \boldsymbol{\gamma}\left[\frac{6(1-\nu)\boldsymbol{a}^4}{E\boldsymbol{h}^5}\right]$
	$\boldsymbol{E}$ = elastic modulus	$p = \boldsymbol{p}\left[\frac{6(1-\nu)\boldsymbol{a}^4}{E\boldsymbol{h}^4}\right]$
	γ = interfacial adhesion energy	$y = \boldsymbol{y}/\boldsymbol{h}$
	$\boldsymbol{p}$ = disjoining pressure	
	$\boldsymbol{y}$ = surface force range	
Mechanical loading	$\boldsymbol{F}$ = applied external force	$F = \boldsymbol{F}\left[\frac{6(1-\nu)\boldsymbol{a}^2}{\pi E\boldsymbol{h}^4}\right]$
	$\boldsymbol{f}$ = applied pressure	$f = \boldsymbol{f}\left[\frac{6(1-\nu)\boldsymbol{a}^4}{E\boldsymbol{h}^4}\right]$

suggest a new parameter similar to μ, and demonstrate its usage in blister tests. For simplicity, all variables used hereafter are normalized as in Table 1. Bold symbols represent the physically measureable quantities.

2. THE JKR-DMT TRANSITION FOR THIN MEMBRANES

An isotropic linear elastic membrane adheres to a rigid substrate *via* intrinsic disjoining pressure at the interface. External load or uniform pressure then drives a delamination at the membrane-substrate interface. No membrane wrinkling is allowed here. For demonstration purposes, a classical energy balance method is adopted here while mode mixity[1] is ignored even though the stretched membrane is likely driven by a shearing mode. Brief derivations are given in the Appendix. The universal JKR-DMT transition parameter, ψ, for a thin flexible membrane possessing zero flexural rigidity and deforming under pure stretching is given by

$$\psi_{\text{stretching}} = \frac{p}{\gamma^{3/4}} = \left[\frac{6(1-\nu)\boldsymbol{a}^4}{\gamma^3 \boldsymbol{E}\boldsymbol{h}}\right]^{1/4} \boldsymbol{p}, \tag{1}$$

with the blister radius, a, and membrane thickness, h, representing membrane geometry (*c.f.*, R in a solid sphere). The membrane behavior transits from JKR to DMT as ψ spans a range of values specific to different blister geometries. For a thick and stiff membrane under pure bending with negligible stretching,

$$\psi_{\text{bending}} = \frac{p}{\gamma^{1/2}} = \left[\frac{6(1-\nu)\boldsymbol{a}^4}{\gamma \boldsymbol{E}\boldsymbol{h}^3}\right]^{1/2} \boldsymbol{p}. \tag{2}$$

Though both $\psi_{\text{stretching}}$ and ψ_{bending} are dimensionless, note their distinct dependencies on the membrane geometry and materials parameters. Three case studies are investigated: (i) the standard pressurized blister test, (ii) the constrained blister test for a clamped membrane, and (iii) the punch test for a radial inward growing delamination. The analysis provides a theoretical tool to interpret future experimental data.

[1]Mode mixity will lead to a modified load-displacement relationship, and membrane profile. The disjoining pressure considered here acts perpendicular to the adhering surfaces. Should mixed opening-shearing be considered, the lateral component of p has to be considered, which is beyond the scope of this paper.

2.1. Case Study 1: The Standard Pressurized Blister Test

Figure 1a shows a blister delamination of radius, c, and height, w_0, driven by a uniform pressure, f, *via* a bore of radius, a, in the substrate. The cohesive zone is shown as $b < r < c$. For a range of disjoining pressure, Figs. 1b and c show the mechanical responses of membranes under pure stretching and pure bending, respectively. All curves are independent of γ. Initial pressurization leads to a small rise in w_0 without delamination until the blister grows beyond the venting hole. Further increase in f expands c. For $w_0 < y$, the entire freestanding membrane remains under the influence of the disjoining pressure that counterbalances the applied pressure and the membrane bounded by the bore is inflated without delamination. Two possible scenarios then follow. If the applied pressure exceeds the total disjoining pressure prior to $w_0 = y$, the membrane will gradually delaminate from the substrate and the force curve $f(w_0)$ is continuous when transiting from inflation to delamination. Conversely, if the applied pressure remains below the disjoining pressure even when w_0 reaches y, delamination will be delayed. When the increasing applied pressure eventually exceeds the disjoining pressure, "pop-in" occurs and the delamination edge spontaneously grows to an equilibrium dimension. A sudden jump is, therefore, expected in $f(w_0)$. For simplicity, we assume hereafter a smooth inflation-delamination transition. The relation $f(w_0)$ is a monotonically increasing function and the delamination process is stable, which is quite unexpected according to the classical *unstable* pressurized blister assuming zero force range [5]. A maximum pressure, $f_{\max}$, is reached when the blister height finally catches up with the surface force range, $w_0 = y$. Further increase in f until $w_0 > y$ renders the cohesive zone residing to an annulus around the contact edge ($b < c$) such that the cohesive zone width ($c - b$) continues to diminish. Hereafter $f(w_0)$ becomes monotonically decreasing, in that, pressure increase leads to an ebbing blister height despite an expanding delamination radius. At $f_{\max}$, the delamination grows spontaneously and catastrophically until it reaches the physical edge of the sample substrate. One possible way to stabilize the blister is to allow a fixed mass of working gas in the blister void while the delamination is driven by reducing the external pressure [16]. The internal pressure drops while the working gas expands.

The long range disjoining pressure manifests itself as follows. For small ψ, the blister height is relatively small because the entire blister lies within the cohesive zone ($b = c$), and $f_{\max}$ is also small. A large ψ approaches the JKR-limit. Here ψ is not well defined since the bore radius, a, is the only fixed dimension other than the membrane

thickness. The a-dependency of ψ becomes negligible as the blister expands outwards beyond the hole ($c >> a$). Nonetheless, increase of ψ from 10 to 100 in Fig. 1b demonstrates the fact that a large ψ approaches the JKR-limit. Besides, the expanding blister forbids the possibility of pull-off as in the other two blister geometries to be discussed in the next sections.

2.2. Case Study 2: The Constrained Blister Test

In the classical constrained blister test (Fig. 2a), the top plate limits the blister height, w_0, to a fixed constant. Increase in f presses the membrane against the top plate into an adhesion contact. Reduction in f, therefore, delaminates the membrane and shrinks the contact circle. The theoretical adhesion-delamination mechanics in the JKR and DMT limits and the associated JKR-DMT transition have been extensively investigated by Dillard *et al.* for both linear and nonlinear elastic plate and membrane under bending or stretching [6]. Experimental investigations and associated theoretical models are recently reported in literature. Xu and Liechti built a Moiré interferometer to map the profile of polyethylene terephthalate (PET) films deformed in a constrained blister configuration, but ignored the nonetheless negligible adhesion at the contact interface [17,18]. Flory *et al.* used the constrained blister test to measure interactions between a soft polymer membrane on a rigid substrate and constructed a theoretical model based on the JKR limit and large deformation instead of small strain in linear elasticity [19]. Hui *et al.* constructed a detailed model based on JKR limit and large deformation [20].

Figure 2b shows the delamination behavior of a membrane under pure stretching obtained by a force balancing method used by Plaut, White and Dillard [6,21]. Raising f from null leads to blister bulging but does not immediately incur adhesion contact because of the weak disjoining pressure. Interfacial adhesion occurs once f exceeds a critical threshold, $f_{\min}$. For $\psi \leq 3$, the adhesion contact starts with one point contact ($c = 0$) and so does delamination upon unloading, reminiscent of the DMT limit. Increase in ψ in this range reduces $f_{\min}/\gamma^{3/4}$ until it reaches 1.23. For $\psi > 3$, the function $c(f)$ shows an infinite slope at $f_{\min}$ with $(dc/df) \to \infty$ and $c(f_{\min}) > 0$, indicating a pull-in where the membrane jumps into adhesion contact at $f_{\min}$. Upon unloading, pull-off is expected at $f_{\min}$ where the membrane spontaneously snaps from the plate, resembling the JKR-limit with $\psi \to \infty$. The JKR-DMT transition is apparent. Figure 2c shows similar behavior for the blister under pure bending. For $\psi \leq 2$, the

delamination process resembles the DMT limit with a point contact ($c = 0$) at the beginning of loading and end of unloading. For $2 < \psi \leq 2000$, decrease in f leads to delamination until the pressure equilibrates on both sides of the membrane with $f = 0$, then the contact circle is arrested with a non-zero radius ($c > 0$). For $\psi > 2000$, the JKR-like pull-off is expected. Note that all the critical values of ψ quoted above and hereafter are only approximations obtained by numerical methods.

2.3. Case Study 3: The Punch Test

The constrained blister test is driven by a uniform pressure that is, in practice, difficult to measure accurately. An alternative is to replace the pressure by a mechanical force that can be gauged by a load cell. Figure 3a shows a circular membrane with radius, a, clamped at the periphery. A cylindrical punch with a planar surface makes adhesion contact with the diaphragm, before a tension is applied to the punch to delaminate the membrane. Simultaneously measuring the applied load, F, punch displacement or blister height, w_0, the contact radius, c, and the membrane profile allows one to deduce the magnitude and range of the disjoining pressure. We collaborated with Dillard to build the adhesion-delamination mechanics in the JKR limit and in the presence of a residual membrane stress [8]. The work was lately extended to the JKR-DMT transition for finite p and y [9]. In our previous work for a thin membrane under pure stretching, the adhesion-delamination mechanics is derived based on an assumption, albeit arbitrary, that the adhesion energy, $\gamma = 1$. Though valid, the new parameter, ψ, takes into account the variation in γ.

Contrasting the force-balancing method in the constrained blister, we adopt an energy balance method for the punch test. Figure 3b shows the mechanical behavior of an initially stress-free membrane. Throughout the loading process, the contact circle continues to shrink (not shown). For $\psi < 1.86121$, the cohesive zone spans the entire freestanding membrane with $b = a$. Delamination proceeds in a stable manner under either fixed load ($F =$ constant) or fixed grips ($w_0 =$ constant), and the membrane ultimately pinches off from the substrate with $c = 0$ at the maximum external load on the dashed curve OD, resembling the DMT limit. For $1.86121 < \psi < 10$, the cohesive zone becomes a shrinking annulus as delamination proceeds ($c < b < a$). After reaching a maximum load, $F_{\max}$, the applied load decreases to maintain equilibrium until the final pinch-off on DC. For $\psi \geq 10$, the contact radius is non-zero ($c \neq 0$) at the final pull-off,

resembling the JKR limit. The full JKR solution becomes apparent in the limit of $\psi \to \infty$. The dashed curve OADCF traces the loci of "pinch-off" and pull-off. Figure 3c shows a similar delamination process for a stiff membrane under pure bending. Transition from DMT to JKR occurs at $\psi = 4.\sqrt{2} \approx 5.657$, where the force curve terminates at D. For $\psi < 5.657$, the DMT limit prevails and the delamination terminates at pinch-off on the dashed curve. A larger ψ raises $F_{\max}$ which indicates the onset of cohesive zone shrinkage. In the limit of $\psi \to \infty$, pull-off dominates in the JKR limit.

3. DISCUSSION

Notwithstanding the similarities in ψ and μ, there are fundamental differences between the two quantities. In bulk solid adhesion, the geometrical incompatibility leads to the classical Hertzian compressive stress within the contact, while interfacial adhesion poses an additional tensile stress at the contact edge as in the JKR limit. The local deformation leads to a "neck" at the contact circle. In fact, the Tabor's parameter was originally derived based on the neck height [12]. In thin film adhesion, as in the three aforementioned blister tests, both the membrane and the substrate are planar and geometrically compatible. There is, therefore, neither compressive stress nor membrane stress present within the adhesion contact. Disjoining pressure alters the deformed membrane profile only in the freestanding annular region behind the delamination front. The width or height of the cohesive zone where the disjoining pressure acts can be referred to as a virtual neck in membrane adhesion.

Another distinction between ψ and μ is that a and h are present in the geometrical factor in ψ [*c.f.*, (a^4/h) in Eq. (1) and (a^4/h^3) in Eq. (2)], compared with the single dimension, R, in μ. The inclusion of h is essential, since it governs not only the JKR-DMT transition, but also the mechanical response from pure plate-bending to membrane-stretching [7,22]. Upon external loading, a membrane undergoes mixed bending-stretching. When the blister height is small compared with membrane thickness, or $w/h < 1$, bending dominates. But when $w/h > 3$, stretching prevails. It is, therefore, expected that ψ should show a transition from ψ_{bending} to $\psi_{\text{stretching}}$ with h playing the role of transition. It is also natural to state that yet another transition is possible as h increases further such that a bending plate thickens to a bulk solid. Derivation of the universal parameter governing adhesion from thin to thick membrane, then from thick film to bulk solid, is beyond the scope of this paper.

Comparative dependences of ψ and μ upon the material factors γ and E deserve further discussion. It is remarkable that $\psi \propto \gamma^{-m}$ with the index m varying from 1/2 to 3/4 (*i.e.*, from bending to stretching) but $\mu \propto \gamma^{-1/3}$. In other words, change in adhesion strength will have a more significant effect on membranes such that a decrease in γ pushes the delamination behavior closer to the JKR limit than does the bulk solid. On the other hand, $\psi \propto E^{-n}$ with $\frac{1}{4} \leq n \leq \frac{1}{2}$, but $\mu \propto E^{-2/3}$. Stiffening of the materials with an increase in E reduces μ to a larger extent than ψ and, therefore, pushes the solid closer to the DMT limit.

The aforementioned blister configurations are axisymmetric. It is possible to derive an alternative ψ for 1-D membranes [23]. In particular, a rectangular membrane can be clamped at the two opposite edges while being subject to a uniform pressure similar to the constrained blister or a rectangular punch under a tensile load. It is tempting to replace the blister diameter, $2a$, by membrane length, $2l$, but it is noted that the adhesion-delamination mechanics is quite different from the 2-D counterpart. For instance, no pull-off is expected for 1-D. Detailed derivation is beyond the scope of this paper.

4. CONCLUSION

We have shown how the new dimensionless parameter ψ is used to gauge the JKR-DMT transition for adhesion-delamination of a thin membrane from a rigid substrate. Table 2 summarizes the critical value of ψ^* where the DMT-JKR transition occurs. The value of ψ^* is difficult to define for the pressurized blister because the blister is ever expanding in dimension and the characteristic pull-off does not occur. For membranes with $\psi > \psi^*$, the behavior approaches the JKR limit, but $\psi < \psi^*$ tends to the DMT limit.

This paper is to honor Professor David A. Dillard for his 3 M Award presented at the 33rd Adhesion Society Annual Meeting & Expo at Daytona Beach, Florida, 21–24, Feb. 2010. His many invaluable contributions to adhesion science are treasured by the adhesion community.

TABLE 2 Critical Value of y for DMT-JKR Transition

	$(\psi_{\text{stretch}})^*$	$(\psi_{\text{bend}})^*$
Constrained blister test	≈ 3	≈ 2
Punch test	1.861	5.657

ACKNOWLEDGMENTS

This work is supported by the National Science Foundation through Grant CMMI # 0757140. Any opinions, findings, and conclusions or recommendations expressed in this material are those of the authors and do not necessarily reflect the views of the National Science Foundation. We are grateful to the reviewers for invaluable comments.

REFERENCES

[1] Chang, Y. S., Lai, Y. H., and Dillard, D. A., *Journal of Adhesion* **27**, 197–211 (1989).
[2] Lai, Y. H. and Dillard, D. A., *Journal of Adhesion* **31**, 177–189 (1990).
[3] Lai, Y. H. and Dillard, D. A., *Journal of Adhesion* **33**, 63–74 (1990).
[4] Dannenberg, H., *Journal of Applied Polymer Science* **5**, 125–134 (1961).
[5] Bennett, S. J., Devries, K. L., and Williams, M. L., *International Journal of Fracture* **10** (1), 33–43 (1974).
[6] Plaut, R. H., White, S. A., and Dillard, D. A., *International Journal of Adhesion and Adhesives* **23**, 207–214 (2003).
[7] Wan, K.-T., *Journal of Applied Mechanics* **69**, 110–116 (2002).
[8] Wan, K.-T. and Dillard, D. A., *Journal of Adhesion* **79**, 123–140 (2003).
[9] Wan, K.-T. and Julien, S. E., *Journal of Applied Mechanics* **76**, 051005, DOI: 10.1115/1.3112745 (2009).
[10] Johnson, K. L., Kendall, K., and Roberts, A. D., *Proceedings of the Royal Society of London A* **324**, 301–313 (1971).
[11] Maugis, D., *Contact, Adhesion, and Rupture of Elastic Solids*, (Springer, New York, 2000).
[12] Tabor, D., *Journal of Colloid and Interface Science* **58** (1), 2–13 (1977).
[13] Muller, V. M., Yushchenko, V. S., and Derjaguin, B. V., *Journal of Colloid and Interface Science* **77** (1), 91–101 (1980).
[14] Maugis, D., *Journal of Colloid and Interface Science* **150**, 243–269 (1992).
[15] Johnson, K. L. and Greenwood, J. A., *Journal of Colloid and Interface Science* **192** (2), 326–333 (1997).
[16] Wan, K.-T. and Mai, Y. W., *Acta metallurgica et materialia* **43** (11), 4109–4115 (1995).
[17] Xu, D. and Liechti, K. M., *Experimental Mechanics* **50** (2), 217–225, DOI: 10.1007/s11340-009-9291-0 (2010).
[18] Xu, D. and Liechti, K. M., *International Journal of Solids and Structures* **47**, 969–977, DOI: 10.1016/j.ijsolstr.2009.12.013 (2010).
[19] Flory, A. L., Brass, D. A., and Shull, K. R., *Journal of Polymer Science Part B: Polymer Physics* **45** (24), 3200–3394, DOI: 10.1002/polb.21322 (2007).
[20] Long, R., Shull, K. R., and Hui, C.-Y., *Journal of Mechanics and Physics of Solids* **58** (9), 1225–1292 (2010).
[21] White, S. A., *The Effect of Work of Adhesion on Contact of a Pressurized Blister with a Flat Surface*, (M.S. Thesis, Virginia Tech, Blacksburg, VA, 2001).
[22] Arjun, A. and Wan, K.-T., *International Journal of Adhesion and Adhesives* **25** (1), 13–18 (2005).
[23] Li, G. and Wan, K.-T., *Journal of Adhesion* **86** (3), 335–351 (2010).

APPENDIX: BRIEF DERIVATION OF THE UNIVERSAL PARAMETER ψ

The flexural rigidity of a membrane is given by $\kappa = Eh^3/12(1-\nu^2)$. In the presence of an external load, the membrane is deformed by mixed bending ($\kappa \cdot \nabla^4 w$) and stretching ($-\sigma h \cdot \nabla^2 w$ with σ the membrane stress), and the membrane profile $w(r)$ is governed by

$$\kappa \cdot \nabla^4 w - \sigma h \cdot \nabla^2 w = p, \quad \text{within the cohesive zone} \tag{A1}$$

$$\kappa \cdot \nabla^4 w - \sigma h \cdot \nabla^2 w = \Omega(r), \quad \text{without the cohesive zone,} \tag{A2}$$

where ∇^2 is the Laplacian operator in cylindrical coordinates, and the loading function is given by $\Omega(r) = f$ for both pressurized and constrained blisters and $\Omega(r) = F \cdot \delta(r)$ for the punch test with the delta function $\delta(r)$ denoting the central load. The cohesive zones are defined to be the interface where the disjoining pressure is active (*c.f.*, Figs. 1a, 2a, and 3a) where $w(b) < y$. Equations (A1–A2) can be recast using the dimensionless variables in Table 1, and solved exactly for the boundary conditions: $w(r)$ being differentiable at the cohesive edge and blister edge. One other condition is $\gamma = py$, which can also be recast in dimensionless form. An energy balance is then obtained by defining the total energy, U_T, as the sum of elastic energy, U_E, and surface energy, U_S. The delamination trajectory is obtained by following the local minimum of U_T or $(dU_T/dc) = 0$, yielding $f(w_0, c)$ or $F(w_0, c)$.

We demonstrated the punch test of a flexible membrane under pure stretching [9]. Since $\kappa = 0$, the term ($\kappa \cdot \nabla^4 w$) in (A1–A2) is ignored. A plot of F *versus* w_0 is obtained for a specific adhesion energy $\gamma = 1$, showing the DMT-JKR transition at $p = 1.86$. Alternatively, when $F/\gamma^{3/4}$ is plotted as a function of $w_0/\gamma^{1/4}$, as in Fig. 3b, the curves for different values of $p/\gamma^{1/4}$ become independent of γ. We, therefore, define $\psi_{\text{stretch}} = p/\gamma^{1/4}$. Equation (1) is obtained by reverting ψ_{stretch} to the physical quantities involved, and Figs. 3b–c then follow. The same procedures are repeated for a bending plate by ignoring ($\sigma h \cdot \nabla^2 w$) in (A1–A2). Again, the mechanical response $F(w_0)$ depends on γ, but a modified plot of $F/\gamma^{1/2}$ *versus* $p/\gamma^{1/2}$ as a function of $p/\gamma^{1/2}$ is independent of γ (Fig. 3c). A new parameter ψ_{bend} is, therefore, defined as in Eq. (2). The universal parameters for pressurized and constrained blisters are similarly derived. The corresponding ψ_{stretch} and ψ_{bend} differ from the punch counterparts by a numerical proportionality constant (*c.f.*, Figs. 1b–c and 2b–c).